



Alexandria University  
**Alexandria Engineering Journal**

[www.elsevier.com/locate/aej](http://www.elsevier.com/locate/aej)  
[www.sciencedirect.com](http://www.sciencedirect.com)



## ORIGINAL ARTICLE

# Natural convection and thermal radiation influence on nanofluid flow over a stretching cylinder in a porous medium with viscous dissipation

Alok Kumar Pandey\*, Manoj Kumar

*Department of Mathematics, Statistics and Computer Science, G.B. Pant University of Agriculture and Technology, Pantnagar 263145, India*

Received 11 July 2016; revised 29 August 2016; accepted 31 August 2016

## KEYWORDS

Nanofluid;  
 Natural convection;  
 Slip boundary conditions;  
 Stretching cylinder;  
 Thermal radiation;  
 Viscous dissipation

**Abstract** The purpose of the present work is to examine the collective influence of thermal radiation and convection flow of Cu-water nanofluid due to a stretching cylinder in a porous medium along with viscous dissipation and slip boundary conditions. The governing non-linear ODEs and auxiliary boundary conditions those obtained by applying assisting similarity transformations have been handled numerically with shooting scheme through Runge-Kutta-integration procedure of fourth-fifth order. The non-dimensional velocity and temperature distribution are designed and also skin friction coefficient as well as heat transfer rate are tabulated for various values of relatable parameters. The results explain that Nusselt number depreciates with boost in radiation parameter, thermal slip parameter and Eckert number. Moreover, it is accelerated with increase in velocity slip parameter and natural convection parameter. The results are distinguished via published ones and excellent accord has been detected.

© 2016 Faculty of Engineering, Alexandria University Published by Elsevier B.V. This is an open access article under the CC BY-NC-ND license (<http://creativecommons.org/licenses/by-nc-nd/4.0/>).

## 1. Introduction

The nanofluid is the amalgamation of suspensions of nano-size particles into the conventional fluids which was firstly pioneered by Choi [1]. The nanoparticles involved in this fluid are made of metals, carbides and oxides or carbon nanotubes, and conventional fluids take account of water, oil and ethylene

glycol. The thermal conductivity of nanoparticles is larger than that of regular fluids, and due to this fact solid particles are used to enhance the thermal properties of base fluids. So the existence of nano solid particles in the conventional fluids heat transfer characteristics enhanced. There are several potential uses of nanofluids in heat transfer such as engine cooling, refrigerator, chiller, microelectronics, and fuel cells. In the analysis of heat transfer enhancement of nanofluid due to solid particles, there are two different approaches, one is single phase model, in which both solid particles and fluids are in thermal equilibrium and this model is simple and expedient for computation and next one is two-phase model, which deals

\* Corresponding author.

E-mail addresses: [mr.alokpandey1@gmail.com](mailto:mr.alokpandey1@gmail.com) (A.K. Pandey), [mnj\\_kumar2004@yahoo.com](mailto:mnj_kumar2004@yahoo.com) (M. Kumar).

Peer review under responsibility of Faculty of Engineering, Alexandria University.

<http://dx.doi.org/10.1016/j.aej.2016.08.035>

1110-0168 © 2016 Faculty of Engineering, Alexandria University Published by Elsevier B.V.

This is an open access article under the CC BY-NC-ND license (<http://creativecommons.org/licenses/by-nc-nd/4.0/>).

Please cite this article in press as: A.K. Pandey, M. Kumar, Natural convection and thermal radiation influence on nanofluid flow over a stretching cylinder in a porous medium with viscous dissipation, Alexandria Eng. J. (2016), <http://dx.doi.org/10.1016/j.aej.2016.08.035>

with the role of solid particles and fluid in heat transfer process.

In the last few years, a lot of engineering function of convective flow in a porous medium such as building erection, solar collectors, ventilation procedure, temperature exchangers, and removal of heat from nuclear reactors. Wang [2] premeditated the steady flow of fluid over a stretching cylinder as of outer surface. The leading problem is a third order ODEs that leads to accurate similitude solutions of the Navier-Stokes equations. The combined effect of MHD and entropy generation flow over a stretching cylinder in the continuation of porous medium was deliberated by Butt et al. [3] they examined that as boost in magnetic parameter and permeability parameter thickness of momentum boundary layer diminishes. Ishak et al. [4] described suction/injection influence on steady flow of an incompressible fluid over a permeable stretching tube. They found that Reynolds number ascends as mounting in the numerical values of skin friction coefficient. Ashorynejad et al. [5] have considered the effect of magnetohydrodynamic flow over a stretching tube within nanofluid. They found that on escalating the values of flow rate both magnetic parameter and Reynolds number are augmented. Ahmed et al. [6] premeditated the joint influence of thermal conductivity, dynamic viscosity and heat source/sink in the existence of stretching permeable tube in nanofluid. Majeed et al. [7] considered the simultaneous impact of partial slip and heat transfer on steady non-Newtonian Casson fluid flow outside of stretching tube with arranged heat flux. They analyzed that as increase in Casson fluid parameter, the heat transfer rate diminishes. Hayat et al. [8] have discussed magnetohydrodynamic third grade fluid flow due to a stretching cylinder. They found that radial velocity decreases on diminishing Reynolds number. The impact of mixed convection steady flow on stretching tube has been proposed by Wang [9]. Si et al. [10] considered the heat transfer influence on unsteady viscous flow over a stretching porous tube. Wang and Ng [11] inspected viscous fluid flow outside of stretching cylinder with slip. They found that on enhancing the values of unsteady parameter temperature of nanoparticle rises. Ishak and Nazar [12] proposed the laminar and incompressible viscous fluid flow due to a stretching cylinder. Naramgari and Sulochana [13] presented the influence of flow and heat transfer on nanofluid flow over a stretching surface with MHD. Sk et al. [14] analyzed the combined influence of MHD and slip on permeable stretching surface in nanofluid. An assortment of studies to expect the influence of thermal radiation on nanofluid flow due to a stretching/shrinking sheet has been offered by [15–18]. Several efforts have been set to scrutinize the influence of natural convection during nanofluid flow under various conditions (see [19–24]). Ganga et al. [25] have discussed the viscous and ohmic dissipation effect on MHD flow over vertical plate with heat generation/absorption in a nanofluid. They established that Nusselt number reduces as diminished in Eckert number. Hayat et al. [26] have introduced the combined effect of Brownian motion and thermophoresis on viscoelastic nanofluid flow due to a stretching cylinder in the presence of mixed convection. The influences of thermal radiation on mixed convection flow over a different geometry were studied by [27–29]. Khan and Malik [30,31] examined the heat transfer flow of Sisko fluid over a stretching cylinder with convective boundary conditions. Very recently, analysis of heat transfer flow of Sisko fluid over a stretching cylinder is studied by [32,33].

Waqas et al. [34] have analyzed the boundary layer flow burger fluid over a stretching sheet with Cattaneo-Christov heat flux model. Again, Waqas et al. [35] investigated the influence MHD flow of micropolar fluid over a stretched surface with convective boundary conditions. Hayat et al. [36] have studied influence of source/sink on mixed convection flow in viscoelastic nanofluid due to a cylinder in the presence of variable thermal conductivity. Recently, influences of MHD flow of nanofluid over a different geometry were presented by [37–41]. The present work deals with the influence of natural convection, viscous dissipation, heat source/sink and thermal radiation on nanofluid steady flow over a stretching porous cylinder in the existence of slip boundary conditions. The numerical solution of the problem is acquired by employing shooting scheme based Runge-Kutta-Fehlberg-integration algorithm.

## 2. Mathematical formulation

Consider an axisymmetric, incompressible, steady, laminar flow of a nanofluid over a flat stretching porous pipe of radius  $b$  and  $(z, r)$  are taken as directions of axis toward horizontal and vertical of the cylinder as depicted in Fig. 1. It is presumed that surface temperature of the pipe is  $T_w$  and temperature far from the surface is  $T_\infty$  where  $(T_w > T_\infty)$ . The ohmic heating, magnetic field, suction/injection and Hall effect are neglected. The regular fluid (water) based nanofluid containing  $Cu$  (Copper) as a nanoparticle is considered. The physical properties of solid particles and regular fluid are mentioned in Table 1.

The primary equation of mass, momentum and energy for this model are articulated as follows (see in Refs. [4–6]):

$$\frac{\partial(rw)}{\partial z} + \frac{\partial(ru)}{\partial r} = 0 \quad (1)$$

$$\rho_{nf} \left( w \frac{\partial w}{\partial z} + u \frac{\partial w}{\partial r} \right) = \mu_{nf} \left( \frac{\partial^2 w}{\partial z^2} + \frac{1}{r} \frac{\partial w}{\partial r} - \frac{w}{k} + \frac{g(\rho\beta)_{nf}}{\mu_{nf}} (T - T_\infty) \right) \quad (2)$$

$$\rho_{nf} \left( w \frac{\partial u}{\partial z} + u \frac{\partial u}{\partial r} \right) = -\frac{\partial p}{\partial r} + \mu_{nf} \left( \frac{\partial^2 u}{\partial r^2} + \frac{1}{r} \frac{\partial u}{\partial r} - \frac{u}{r^2} \right) \quad (3)$$

$$(\rho C_p)_{nf} \left( w \frac{\partial T}{\partial z} + u \frac{\partial T}{\partial r} \right) = \left[ k_{nf} \left( \frac{\partial^2 T}{\partial r^2} + \frac{1}{r} \frac{\partial T}{\partial r} \right) + Q_0 (T - T_\infty) - \frac{\partial q_r}{\partial r} + \mu_{nf} \left( \frac{\partial w}{\partial r} \right)^2 \right] \quad (4)$$

The velocity and temperature coupled boundary conditions are [4–6] as follows:

$$\left. \begin{aligned} u = U_w = 0, \quad w = W_w + L \frac{\partial w}{\partial r}, \quad T = T_w + l \frac{\partial T}{\partial r} \quad \text{at } r = b, \\ u \rightarrow 0, \quad T \rightarrow T_\infty \quad \text{as } r \rightarrow \infty \end{aligned} \right\} \quad (5)$$

where  $L$  and  $l$  are the velocity and thermal slip factor, and  $(w, u)$  are the constituent of velocity along with  $(z, r)$  axes respectively. The effective dynamic viscosity  $\mu_{nf}$ , the effective density  $\rho_{nf}$ , the thermal diffusivity  $\alpha_{nf}$ , the heat capacitance  $(\rho C_p)_{nf}$ , the thermal expansion coefficient  $(\beta_{nf})$ , and the thermal conductivity  $k_{nf}$  of the Cu-water nanofluid are defined as follows (see [5]):

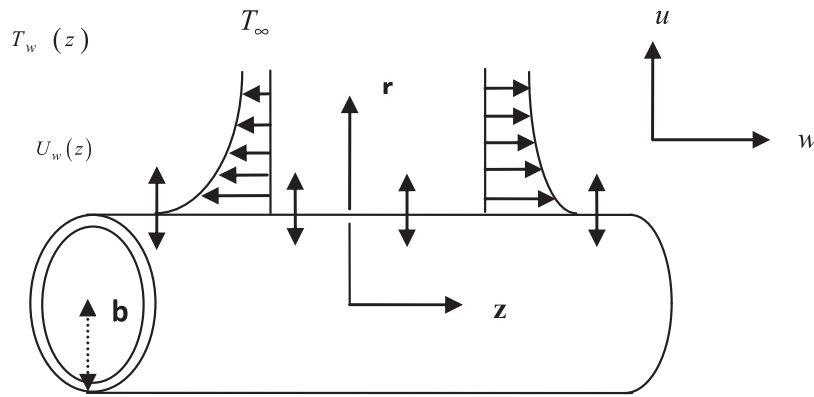


Figure 1 Physical model and geometrical representation.

Table 1 Thermophysical properties of water and Cu-nanoparticles (see Refs. [5] and [6]).

Physical properties	$\rho$ (kg/m <sup>3</sup> )	$C_p$ (J/kgK)	$\beta \times 10^{-5}$ (K <sup>-1</sup> )	$\kappa$ (W/mK)
Pure water	997.1	4179	21	0.613
Copper (Cu)	8933	385	1.67	401

$$\mu_{nf} = \frac{\mu_{bf}}{(1 - \phi)^{2.5}}, \tag{6}$$

$$\rho_{nf} = (1 - \phi)\rho_{bf} + \phi\rho_{sp}, \tag{7}$$

$$\alpha_{nf} = \frac{k_{nf}}{(\rho C_p)_{nf}}, \tag{8}$$

$$(\rho C_p)_{nf} = (1 - \phi)(\rho C_p)_{bf} + \phi(\rho C_p)_{sp} \tag{9}$$

$$\frac{k_{nf}}{k_{bf}} = \frac{k_{sp} + 2k_{bf} - 2\phi(k_{bf} - k_{sp})}{k_{sp} + 2k_{bf} + \phi(k_{bf} - k_{sp})} \tag{10}$$

$$(\rho\beta)_{nf} = (1 - \phi)\rho_{bf}\beta_{bf} + \phi\rho_{sp}\beta_{sp} \tag{11}$$

where  $\phi$ , be the solid volume fraction. The subscripts ( $sp$ ,  $bf$ ) symbolize the nano-solid particles and regular fluid respectively.

The radiative heat flux  $q_r$ , is considered as in  $r$ -direction while it is vanishing toward  $z$ -direction. Therefore, according to Rosseland approximation, the radiative heat flux  $q_r$ , is expressed as [17] follows:

$$q_r = -\frac{16\sigma^* T_0^3}{3k^*} \frac{\partial T}{\partial r} \tag{12}$$

where ( $\sigma^*$ ,  $k^*$ ) are Stefan-Boltzmann constant and coefficient of mean absorption, respectively.

The ensuing non-dimensional similarity transformations have been invoked (Refs. [4–6]):

$$u = -\frac{cb}{\sqrt{\eta}} f(\eta), \eta = \left(\frac{r}{b}\right)^2, w = 2zcf'(\eta), \tag{13}$$

$$\theta(\eta) = \frac{T - T_\infty}{T_w - T_\infty}, \Delta T = T_w - T_\infty,$$

Now putting Eqs. (6)–(13) into Eqs. (2) and (4), respectively, we get the following system of coupled non-linear ODEs [4–6]:

$$\eta f''' + f'' - \lambda f' + A_1 \gamma \theta + A Re (ff'' - f'^2) = 0$$

$$\left(\frac{k_{nf}}{k_f} + \frac{4}{3} Nr\right) \eta \theta'' + \left(\frac{k_{nf}}{k_f} + \frac{4}{6} Nr\right) \theta' + Q_0 \theta + (1 - \phi)^{-2.5} Pr Ec \eta f'^2 + B Pr Re f \theta' = 0 \tag{15}$$

The appropriate boundary conditions (5) in terms of  $f$ , and  $\theta$  become [4–6]

$$\left. \begin{aligned} f'(1) = 1 + sf''(1), f(1) = 0, \theta(1) = 1 + t\theta'(1) \text{ at } \eta = 1 \\ f'(\infty) \rightarrow 0, \theta(\infty) \rightarrow 0 \text{ at } \eta \rightarrow \infty \end{aligned} \right\} \tag{16}$$

where prime designates derivative with respect to  $\eta$ , and  $s$  and  $t$  are the velocity slip and thermal slip parameter. The dimensionless parameters are as follows:  $Pr$  be the Prandtl number,  $\gamma$  be the natural convection parameter,  $\lambda$  be the porous parameter,  $Ec$  be the Eckert number,  $Nr$  be the radiation parameter,  $Re_{bf}$  be the local Reynolds number of the regular fluid,  $Q$  is the heat generation/absorption parameter, and  $A, A_1, B$  are the constants respectively.

$$\lambda = \frac{b^2}{4K}, \gamma = \frac{\beta_{bf} g b^2 \Delta T}{8z c v_{bf}}, Ec = \frac{4\rho_{bf} c^2 z^2}{(\rho C_p)_{bf} \Delta T}, Nr = \left(\frac{4T_\infty^3 \sigma^*}{k_{bf} k^*}\right),$$

$$Pr = \frac{v_{bf}}{\alpha_{bf}}, Q = \frac{Q_0 b^2}{4k_{bf}}, Re = \frac{cb^2}{2v_{bf}},$$

$$A = (1 - \phi)^{2.5} \left[ 1 - \phi + \phi \left(\frac{\rho_{sp}}{\rho_{bf}}\right) \right],$$

$$A_1 = (1 - \phi)^{2.5} \left[ 1 - \phi + \phi \left(\frac{\rho\beta}_{\rho\beta}\right)_{sp} \right],$$

$$B = \left[ 1 - \phi + \phi \left(\frac{\rho C_p}_{\rho C_p}\right)_{sp} \right], \tag{17}$$

It is noticed that the problem can be related to the two dimensional stretching flat surface under the consideration of very large value of Reynolds number ( $Re \gg 1$ ), and Eq. (14) converted to that given by [2,11], when  $\gamma = 0, \lambda = 0, A_1 = 1, A = 1$ .

For the practical interest the substantial quantities, the skin friction coefficient and the local Nusselt number are delineated as follows:

$$C_f = \frac{2\mu_{nf}}{W^2 \rho_{bf}} \left( \frac{\partial w}{\partial r} \right)_{r=b}, Nu = \left( \frac{-bk_{nf}}{\Delta T k_{bf}} \right) \left( \frac{\partial T}{\partial r} \right)_{r=b}. \tag{18}$$

Now, using Eq. (13) in Eq. (18), the non-dimensional skin friction coefficient and the Nusselt number are improved into dimensionless reduced skin friction coefficient and reduced Nusselt number, respectively:

$$(zRe/b)C_f = (\mu_{nf}/\mu_{bf})f''(1), Nu = -(2k_{nf}/k_{bf})\theta'(1). \tag{19}$$

### 3. Numerical method

The non-dimensional momentum equation (14) and energy equation (15) along with assisting boundary conditions (16) have been tackled numerically through shooting scheme with RKF 4–5th order of integration procedure. For this plan, we first alter the primary differential equations into a set of first order ODEs.

Let us consider  $y_1 = \eta, y_2 = f, y_3 = f', y_4 = f'', y_5 = \theta, y_6 = \theta'$ .

Now the following first order system is obtained:

$$\begin{pmatrix} y_1' \\ y_2' \\ y_3' \\ y_4' \\ y_5' \\ y_6' \end{pmatrix} = \begin{pmatrix} 1 \\ y_3 \\ y_4 \\ \frac{\lambda y_3 - y_4 - A_1 \gamma y_5 + A Re (y_3^2 - y_2 y_4)}{y_1} \\ y_6 \\ \frac{-Q y_5 - (1 - \phi)^{-2.5} Pr Ec \gamma_1 y_4^2 - B Re Pr \gamma_2 y_6 - y_6 [(k_{nf}/k_{bf}) + (4/6)Nr]}{\left( \frac{k_{nf}}{k_{bf}} + \frac{4}{3}Nr \right) y_1} \end{pmatrix} \tag{20}$$

and analogous initial conditions:

$$\begin{pmatrix} y_1 \\ y_2 \\ y_3 \\ y_4 \\ y_5 \\ y_6 \end{pmatrix} = \begin{pmatrix} 1 \\ 0 \\ 1 + sg_1 \\ g_1 \\ 1 + tg_2 \\ g_2 \end{pmatrix} \tag{21}$$

The System of first order ODEs (20) along with initial conditions (21) is solved using order of fourth-fifth RKF-integration procedure and appropriate values of unidentified initial conditions  $g_1, g_2$  are selected and then numerical integration is applied. Here we contrast the computed values of  $f'$ , and  $\theta$  as  $\eta = 6(say)$ , through the specified boundary condition  $f'(6) = 0$  and  $\theta(6) = 0$ , and change the estimated values of  $g_1$ , and  $g_2$  to acquire a better approximation for results. The unknown  $g_1$ , and  $g_2$  have been approximated by Newton's scheme such a way that boundary conditions hold at highest numerical values of  $\eta = \infty$ , with error less than  $10^{-8}$ .

### 4. Results and discussion

The solution of altered ODEs (14) and (15) with related boundary conditions (16) was acquired with the aid of RKF scheme via shooting procedure. In order to substantiate the exactitude of our consequence, we have contrasted results with those obtained by Wang [2], Ishak et al. [4] and Ahmed et al. [6] and found that they are in better concord, as revealed in Table 2. The impact of several prevailing physical parameters such as convection parameter ( $\gamma$ ), porous medium parameter ( $\lambda$ ), thermal radiation parameter ( $Nr$ ), velocity slip parameter ( $s$ ), thermal slip parameter ( $t$ ), and Eckert number ( $Ec$ ), heat generation/absorption parameter ( $Q$ ), on flow and heat transfer are elucidated through figures and tables with preset mesh range  $\Delta\eta = 0.001$ , where  $1 \leq \eta \leq 6$  and concentration of solid particle is  $\phi = 0.01$ . The numerical value of constants becomes  $A = 1, A_1 = 1, B = 1$ , for base fluid ( $\phi = 0$ ). Table 3 points out the change in absolute values of skin friction coefficient and heat transfer rate of Cu-water nanofluid for employing parameters as stated above. The effects of distinct governing parameters on velocity and temperature of nanoparticles are revealed in Figs. 2–14 and these graphs assure the boundary conditions (5) and (16) asymptotically. In the current study we have taken Cu like a nanoparticle and water as a regular fluid.

The effect of velocity and thermal slip parameter on velocity of Cu-water nanofluid are depicted in Figs. 2 and 3, respectively for the fixed values of  $Pr = 7, Re = 5, Nr = Q = 0.1, \gamma = \lambda = 2, \phi = 0.01$ , and  $Ec = 0.3$ . It is clarified from Fig. 2 that on enhancing the values of velocity slip parameter, velocity of nanofluid continuously reduces in the range of  $1 \leq \eta < 2.5$ , and for this reason boundary layer width depreciates. Fig. 3 reveals that velocity of the fluid is reduced, as accelerate the values of thermal radiation parameter.

Fig. 4 shows the alteration in velocity graph corresponding to variable  $\eta$ , for several values of natural convection parameter  $\gamma$ , when the existing parameters take the values as such  $Pr = 7, Re = 5, Nr = Q = s = 0.1, Ec = \lambda = 0.2$ , and  $t = 1$ . From this outline, it is perceived that velocity of nanofluid is an escalating function of convection parameter. Table 3, shows that absolute value of skin friction coefficient has been reduced with increase in convection parameter. The graph of flow field versus horizontal axis  $\eta$ , has been illustrated in Fig. 5 of diverse values of porosity parameter  $\lambda$ , at  $Pr = 7, Re = 5, Nr = Q = s = 0.1, Ec = 0.2, \gamma = 2$ , and  $t = 1$ , in the region ( $1 \leq \eta \leq 4.5$ ). It is seen that from this profile, on increasing the values of porosity parameter, velocity of existing fluid decelerates and consequently boundary layer thickness diminishes. From Table 3, it is seen that skin factor is an increasing function of porosity parameter. Fig. 6 has been plotted to examine the nature of velocity of nanofluid corresponding to variable  $\eta$ , for various values of Eckert number, when  $Pr = 7, Re = 5, Nr = s = Q = 0.1, \gamma = \lambda = 2$ , and  $t = 1$ . This graph elucidates that velocity gradient increases with Eckert number.

The variation in velocity profile of Cu-water nanofluid with  $\eta$ , in domain [1, 6), of numerous values of thermal radiation parameter  $Nr$ , is mentioned in Fig. 7 for  $Pr = 7, Re = 5, s = 0.1, t = 1, \gamma = \lambda = 2, Ec = 0.3$ , and  $Q = -2$ . From this profile, as augmented in the radiation parameter, momentum

**Table 2** Comparison of numerous values of Nusselt number  $-\theta'(1)$ , for regular fluid (water) and  $Re = 10, \lambda = 0, \gamma = 0, Nr = 0, Q = 0, s = 0, t = 0, A = 1, A_1 = 1, B = 1$ .

$Pr$	Wang [2]	Ishak et al. [4]	Ahmed et al. [6]	Present study
0.7	1.568	1.5683	1.58679	1.58679
2	3.035	3.0360	3.03553	3.03534
7	6.160	6.1592	6.15776	6.15590
10	10.77	7.4668	7.46419	7.46230

**Table 3** Several values of skin friction coefficient and Nusselt number when  $Pr = 7$  and  $Re = 5$ .

$s$	$t$	$\gamma$	$\lambda$	$Ec$	$Nr$	$Q$	$f''(1)$	$-\theta'(1)$
0	1	2	2	0.3	0.1	0.1	-2.70533	0.43402119
0.1							-1.9945238	0.540229
0.2	1						-1.5961809	0.588924
0.1	0						-1.888999	2.51732
	0.1						-1.9245424	1.8389077
	1					0.1	-1.9945238	0.540229
						-2	-2.0059241	0.572788
						-0.1	-1.995709	0.543609
						0	-1.995119	0.541928
						0.5	-1.9920871	0.533274
						2	-1.98181949	0.5043929
					0.3	-2	-1.9983009	0.567959
					0.5		-1.9908892	0.562299
					1		-1.9733252	0.546987
					2		-1.9421299	0.517441
					5		-1.87625958	0.4530397
0.1	1	2	2	0.3	0.1	0.1	-1.9945238	0.540229
				0.4			-1.97002999	0.46609975
				0.6			-1.9227949	0.323763
		0.2	0.2	0.2			-1.863332	0.64331
		1					-1.826313	0.64675
		2					-1.78134	0.65079
		3					-1.7376549	0.65457
0.1	1	2	0.5	0.2	0.1	0.1	-1.8250124	0.644621
			1				-1.89390996	0.6347767
			2				-2.01965320	0.616503
			3				-2.132620929	0.59974839

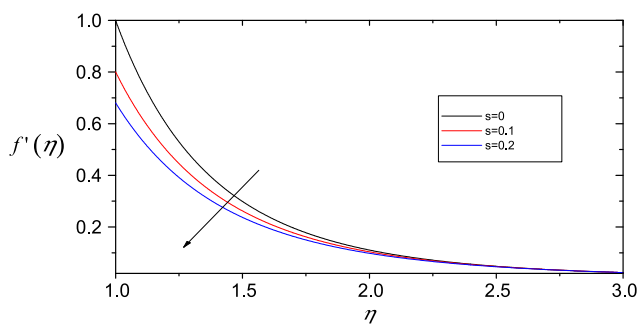


**Figure 2** Velocity profiles for numerous values of  $s$ .

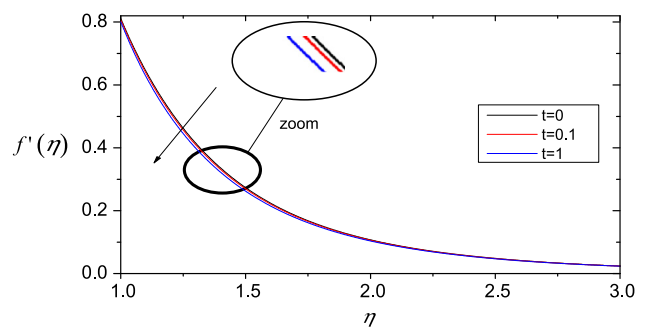


**Figure 3** Velocity profiles for numerous values of  $t$ .

boundary layer thickness accelerates, as well as, tendency of velocity of Cu-water nanofluid enhances.

Figs. 8–14 depict the temperature distribution of employing parameters corresponding to each value of variable  $\eta$ . In Fig. 8, the dual nature of temperature profile is noticed, and

initially it reduces as increasing in velocity slip parameter in region ( $1 \leq \eta \leq 1.6$ ), then after temperature graphs boost with an increase in velocity slip parameter within the domain [1.6, 2.5). Table 3 shows that as increase in the values of velocity slip factor, absolute values of skin friction coefficient

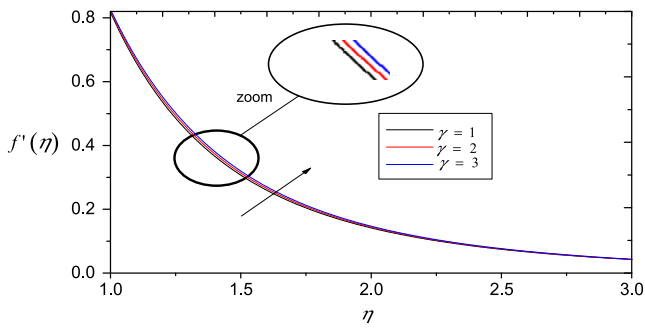


Figure 4 Velocity profiles for numerous values of  $\gamma$ .

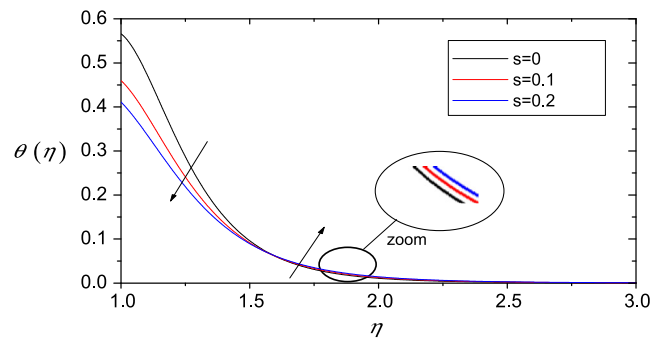


Figure 8 Temperature profiles for numerous values of  $s$ .

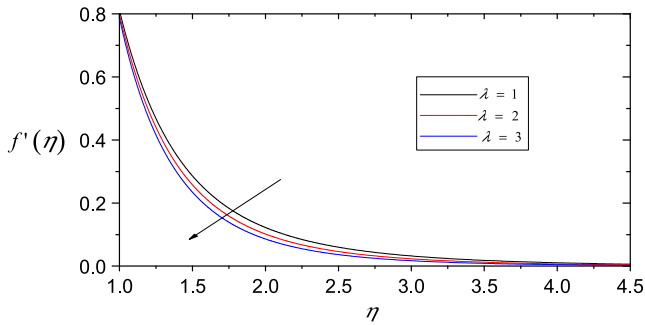


Figure 5 Velocity profiles for numerous values of  $\lambda$ .

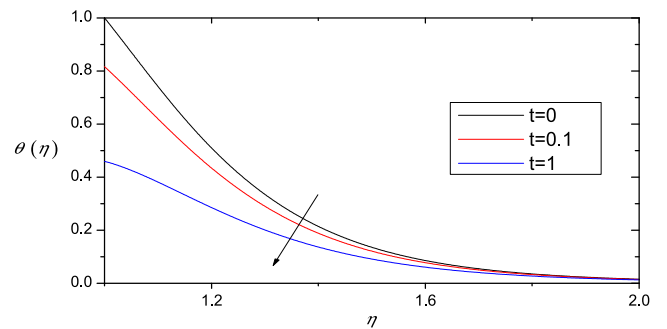


Figure 9 Temperature profiles for numerous values of  $t$ .

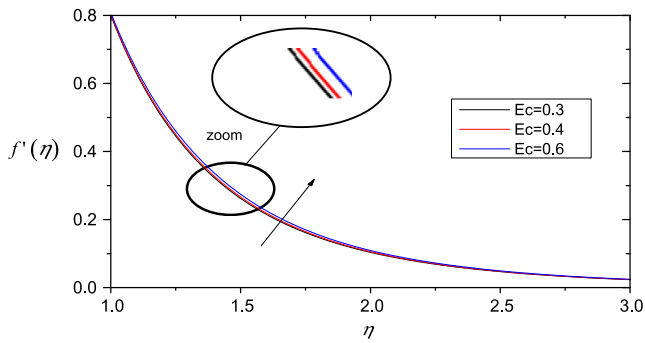


Figure 6 Velocity profiles for numerous values of  $Ec$ .

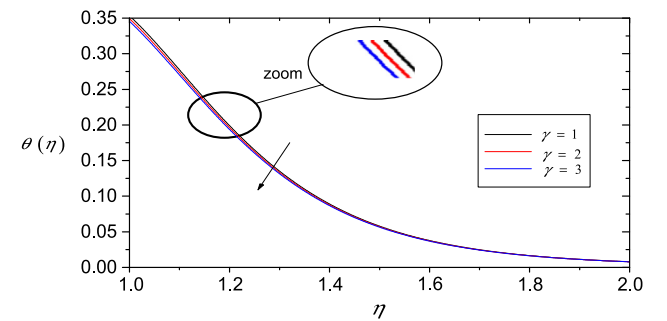


Figure 10 Temperature profiles for numerous values of  $\gamma$ .

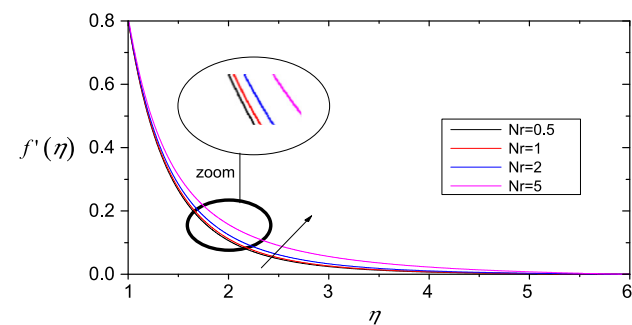


Figure 7 Velocity profiles for numerous values of  $Nr$ .

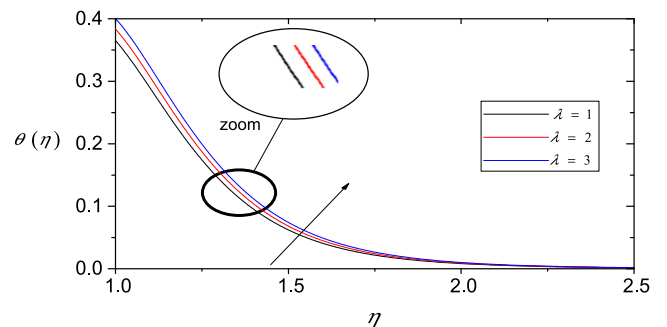


Figure 11 Temperature profiles for numerous values of  $\lambda$ .

diminish but opposite trend is observed for heat transfer rate. According to Fig. 9, on enhancing the values of thermal slip parameter, temperature profile of nanofluid reduces along with

thermal boundary layer thickness. Also, from Table 3, absolute value of rate of flow is accelerated, while, Nusselt number reduces as raised in thermal slip parameter.

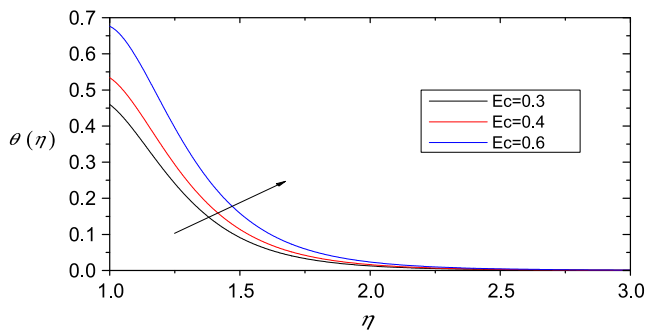


Figure 12 Temperature profiles for numerous values of  $Ec$ .

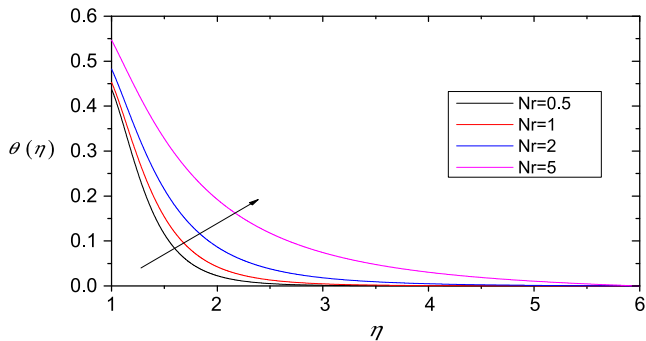


Figure 13 Temperature profiles for numerous values of  $Nr$ .

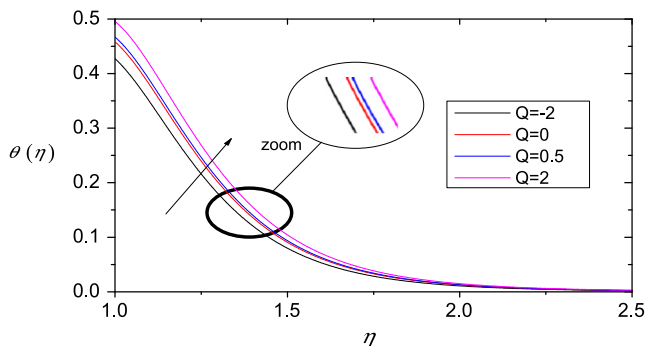


Figure 14 Temperature profiles for numerous values of  $Q$ .

Similarly, Fig. 10 demonstrates that temperature of the fluid reduces with increase in convection parameter. Table 3 reveals that Nusselt number enhances with natural convection parameter. However, Fig. 11 explicates that as increase in porosity parameter, temperature profile increases, and due to this cause thermal boundary layer width accelerates. The deviation in heat transfer rate with porosity parameter is illustrated in Table 3. It is to point out that Nusselt number declines with magnification in porosity parameter.

The variation in temperature profile with respect to variable  $\eta$ , is depicted in Fig. 12, for some values of Eckert number. It is noticed that thermal boundary layer width and temperature graph are accelerated as augmented in Eckert number; moreover, both skin friction and heat transfer rate are decelerated, as enhanced in Eckert number. In the same way, Influence of radiation parameter, on temperature profile is located in

Fig. 13 and it is clarified that temperature of nanofluid is augmented with radiation parameter. It is observed from Table 3, rate of flow and heat transfer rate are simultaneously reduced as augmented in the values of radiation parameter. The impact of heat generation/absorption parameter on temperature profiles of fluid is depicted in Fig. 14. This graph declares that thermal boundary layer thickness escalates along with heat generation/absorption parameter. Moreover, Table 3 illustrates that absolute values of skin factor and Nusselt number decline with an increase in heat generation/absorption parameter.

## 5. Conclusions

The simultaneous consequence of natural convection, thermal radiation and viscous dissipation effect on outside flow over a stretching cylindrical porous pipe in the presence of slip boundary conditions utilized nanofluid (Cu-water) has been analyzed and studied. The solution of ODEs with boundary conditions has been acquired by applying RKF-integration technique via shooting procedure. The authors concluded that following:

- Velocity profile of nanofluid enhances with natural convection parameter, while temperature profile diminishes as increase in the values of natural convection parameter.
- Absolute value of skin friction coefficient escalates with increase in porosity parameter, moreover, Nusselt number reduces as increase in porosity parameter.
- On escalating the values of thermal slip parameter, temperature of Cu-water nanofluid reduces.
- Heat transfer rate augments with escalation in velocity slip parameter, thermal radiation and Eckert number.
- The absolute value of skin friction coefficient reduces as augmented in the numerical values of heat generation/absorption and thermal radiation.

## Acknowledgements

The authors wish to convey their genuine thanks to the reviewers for their essential suggestions and comments to progress the superiority of this manuscript. This research did not receive any specific grant from funding agencies in the public, commercial, or for-profit sectors.

## References

- [1] S.U.S. Choi (Ed.), *Enhancing Thermal Conductivity of Fluids with Nanoparticles*, vol. 231, ASME Publications-Fed, 1995, pp. 99–106.
- [2] C.Y. Wang, Fluid flow due to a stretching cylinder, *Phys. Fluids* 31 (3) (1988) 466–468.
- [3] A.S. Butt, A. Ali, A. Mehmood, Numerical investigation of magnetic field effects on entropy generation in viscous flow over a stretching cylinder embedded in a porous medium, *Energy* 99 (2016) 237–249.
- [4] A. Ishak, R. Nazar, I. Pop, Uniform suction/blowing effect on flow and heat transfer due to a stretching cylinder, *Appl. Math. Model.* 32 (10) (2008) 2059–2066.
- [5] H.R. Ashorynejad, M. Sheikholeslami, I. Pop, D.D. Ganji, Nanofluid flow and heat transfer due to a stretching cylinder in

- the presence of magnetic field, *Heat Mass Transf.* 49 (3) (2013) 427–436.
- [6] S.E. Ahmed, A.K. Hussein, H.A. Mohammed, S. Sivasankaran, Boundary layer flow and heat transfer due to permeable stretching tube in the presence of heat source/sink utilizing nanofluids, *Appl. Math. Comput.* 238 (2014) 149–162.
- [7] A. Majeed, T. Javed, A. Ghaffari, M.M. Rashidi, Analysis of heat transfer due to stretching cylinder with partial slip and prescribed heat flux: a Chebyshev Spectral Newton Iterative Scheme, *Alexandria Eng. J.* 54 (4) (2015) 1029–1036.
- [8] T. Hayat, A. Shafiq, A. Alsaedi, MHD axisymmetric flow of third grade fluid by a stretching cylinder, *Alexandria Eng. J.* 54 (2) (2015) 205–212.
- [9] C.Y. Wang, Natural convection on a vertical stretching cylinder, *Commun. Nonlin. Sci. Numer. Simul.* 17 (3) (2012) 1098–1103.
- [10] X. Si, L. Li, L. Zheng, X. Zhang, B. Liu, The exterior unsteady viscous flow and heat transfer due to a porous expanding stretching cylinder, *Comput. Fluids* 105 (2014) 280–284.
- [11] C.Y. Wang, C.O. Ng, Slip flow due to a stretching cylinder, *Int. J. Non-Linear Mech.* 46 (9) (2011) 1191–1194.
- [12] A.M. Ishak, R.M. Nazar, Laminar boundary layer flow along a stretching cylinder, *Eur. J. Sci. Res.* 36 (1) (2009) 22–29.
- [13] S. Naramgari, C. Sulochana, MHD flow of dusty nanofluid over a stretching surface with volume fraction of dust particles, *Ain Shams Eng. J.* 7 (2) (2016) 709–716.
- [14] M.T. Sk, K. Das, P.K. Kundu, Effect of magnetic field on slip flow of nanofluid induced by a non-linear permeable stretching surface, *Appl. Therm. Eng.* 104 (2016) 758–766.
- [15] D. Pal, G. Mandal, K. Vajravelu, Flow and heat transfer of nanofluids at a stagnation point flow over a stretching/shrinking surface in a porous medium with thermal radiation, *Appl. Math. Comput.* 238 (2014) 208–224.
- [16] A.K. Hakeem, N.V. Ganesh, B. Ganga, Magnetic field effect on second order slip flow of nanofluid over a stretching/shrinking sheet with thermal radiation effect, *J. Magn. Magn. Mater.* 381 (2015) 243–257.
- [17] T. Hayat, T. Muhammad, A. Alsaedi, M.S. Alhuthali, Magnetohydrodynamic three-dimensional flow of viscoelastic nanofluid in the presence of nonlinear thermal radiation, *J. Magn. Magn. Mater.* 385 (2015) 222–229.
- [18] M.R. Krishnamurthy, B.C. Prasannakumara, B.J. Gireesha, R. S.R. Gorla, Effect of chemical reaction on MHD boundary layer flow and melting heat transfer of Williamson nanofluid in porous medium, *Eng. Sci. Technol. Int. J.* 19 (1) (2016) 53–61.
- [19] M. Corcione, M. Cianfrini, A. Quintino, Enhanced natural convection heat transfer of nanofluids in enclosures with two adjacent walls heated and the two opposite walls cooled, *Int. J. Heat Mass Transf.* 88 (2015) 902–913.
- [20] J. Ravnik, L. Škerget, A numerical study of nanofluid natural convection in a cubic enclosure with a circular and an ellipsoidal cylinder, *Int. J. Heat Mass Transf.* 89 (2015) 596–605.
- [21] M. Sheikholeslami, R. Ellahi, Three dimensional mesoscopic simulation of magnetic field effect on natural convection of nanofluid, *Int. J. Heat Mass Transf.* 89 (2015) 799–808.
- [22] A. Mahmoudi, I. Mejri, M.A. Abbassi, A. Omri, Analysis of MHD natural convection in a nanofluid-filled open cavity with non uniform boundary condition in the presence of uniform heat generation/absorption, *Powder Technol.* 269 (2015) 275–289.
- [23] M. El Abdallaoui, M. Hasnaoui, A. Amahmid, Numerical simulation of natural convection between a decentered triangular heating cylinder and a square outer cylinder filled with a pure fluid or a nanofluid using the lattice Boltzmann method, *Powder Technol.* 277 (2015) 193–205.
- [24] B. Mliki, M.A. Abbassi, A. Omri, B. Zeghamati, Augmentation of natural convective heat transfer in linearly heated cavity by utilizing nanofluids in the presence of magnetic field and uniform heat generation/absorption, *Powder Technol.* 284 (2015) 312–325.
- [25] B. Ganga, S.M.Y. Ansari, N.V. Ganesh, A.A. Hakeem, MHD radiative boundary layer flow of nanofluid past a vertical plate with internal heat generation/absorption, viscous and ohmic dissipation effects, *J. Nigerian Math. Soc.* 34 (2) (2015) 181–194.
- [26] T. Hayat, M.B. Ashraf, S.A. Shehzad, N.N. Bayomi, Mixed convection flow of viscoelastic nanofluid over a stretching cylinder, *J. Braz. Soc. Mech. Sci. Eng.* 37 (3) (2015) 849–859.
- [27] T. Hayat, M.B. Ashraf, S.A. Shehzad, A. Alsaedi, Mixed convection flow of Casson nanofluid over a stretching sheet with convectively heated chemical reaction and heat source/sink, *J. Appl. Fluid Mech.* 8 (4) (2015) 803–813.
- [28] M.B. Ashraf, T. Hayat, A. Alsaedi, Radiative mixed convection flow of an Oldroyd-B fluid over an inclined stretching surface, *J. Appl. Mech. Tech. Phys.* 57 (2) (2016) 317–325.
- [29] M. Khan, R. Malik, A. Munir, Mixed convective heat transfer to Sisko fluid over a radially stretching sheet in the presence of convective boundary conditions, *AIP Adv.* 5 (8) (2015) 087178, <http://dx.doi.org/10.1063/1.4929832>.
- [30] M. Khan, R. Malik, Forced convective heat transfer to Sisko fluid flow past a stretching cylinder, *AIP Adv.* 5 (12) (2015) 127202, <http://dx.doi.org/10.1063/1.4937346>.
- [31] M. Khan, R. Malik, Forced convective heat transfer to Sisko nanofluid past a stretching cylinder in the presence of variable thermal conductivity, *J. Mol. Liq.* 218 (2016) 1–7.
- [32] M. Khan, R. Malik, M. Hussain, Nonlinear radiative heat transfer to stagnation-point flow of Sisko fluid past a stretching cylinder, *AIP Adv.* 6 (5) (2016) 055315, <http://dx.doi.org/10.1063/1.4950946>.
- [33] R. Malik, M. Khan, M. Mushtaq, Cattaneo-Christov heat flux model for Sisko fluid flow past a permeable non-linearly stretching cylinder, *J. Mol. Liq.* 222 (2016) 430–434.
- [34] M. Waqas, T. Hayat, M. Farooq, S.A. Shehzad, A. Alsaedi, Cattaneo-Christov heat flux model for flow of variable thermal conductivity generalized Burgers fluid, *J. Mol. Liq.* 220 (2016) 642–648.
- [35] M. Waqas, M. Farooq, M.I. Khan, A. Alsaedi, T. Hayat, T. Yasmeen, Magnetohydrodynamic (MHD) mixed convection flow of micropolar liquid due to nonlinear stretched sheet with convective condition, *Int. J. Heat Mass Transf.* 102 (2016) 766–772.
- [36] T. Hayat, M. Waqas, S.A. Shehzad, A. Alsaedi, Mixed convection flow of viscoelastic nanofluid by a cylinder with variable thermal conductivity and heat source/sink, *Int. J. Numer. Methods Heat Fluid Flow* 26 (1) (2016) 214–234.
- [37] T. Hayat, M. Waqas, S.A. Shehzad, A. Alsaedi, A model of solar radiation and Joule heating in magnetohydrodynamic (MHD) convective flow of thixotropic nanofluid, *J. Mol. Liq.* 215 (2016) 704–710.
- [38] T. Hayat, M. Waqas, M.I. Khan, A. Alsaedi, Analysis of thixotropic nanomaterial in a doubly stratified medium considering magnetic field effects, *Int. J. Heat Mass Transf.* 102 (2016) 1123–1129.
- [39] T. Hayat, M. Waqas, S.A. Shehzad, A. Alsaedi, On model of Burgers fluid subject to magneto nanoparticles and convective conditions, *J. Mol. Liq.* 222 (2016) 181–187.
- [40] T. Hayat, M.I. Khan, M. Waqas, T. Yasmeen, A. Alsaedi, Viscous dissipation effect in flow of magnetonanofluid with variable properties, *J. Mol. Liq.* 222 (2016) 47–54.
- [41] T. Hayat, M.I. Khan, M. Waqas, A. Alsaedi, T. Yasmeen, Diffusion of chemically reactive species in third grade flow over an exponentially stretching sheet considering magnetic field effects, *Chinese J. Chem. Eng.* (2016), <http://dx.doi.org/10.1016/j.cjche.2016.06.008>.